



A simple intra-beam alignment setup for tiled grating assembly based laser pulse compressor of high energy ultrashort pulse laser systems

A K SHARMA^{1,2},

¹Laser Technology Division, Raja Ramanna Centre for Advanced Technology, Indore 452013, India

²Homi Bhabha National Institute, Mumbai 400094, India

e-mail: aksharma@rrcat.gov.in

MS received 21 December 2021; revised 10 February 2023; accepted 15 April 2023

Abstract. Alignment studies on tiled grating assembly (TGA), using pulsed spectrally broadband intra-beam, are reported for tiled grating pulse disperser of a chirped pulse amplification based high energy laser system. Spatial and spectrally resolved far-field profilometry coupled with spatio-spectral interferometry have been used to obtain quantitative values of tip, tilt, in-plane rotation, and piston without ambiguity. Prior to application of present diagnostic setup for coherent phase locking of TGA, point diffractometry has been used for coarse alignment of TGA. Experiment has been carried out using a cw mode-locked femtosecond laser oscillator delivering 200 fs duration laser pulses at 1056 nm. Experimental setup has also been used to estimate groove-density mismatch of gratings for operation and maintenance situations requiring replacement of any grating.

Keywords. Laser pulse compression; diffraction holographic gratings; phase array gratings; groove density errors.

1. Introduction

Ultra-short pulse high energy laser systems are required to study physical processes involved in laser-plasma interaction, generating secondary sources of radiation (*e.g.* THz to gamma rays), charged and neutral particles for various applications [1–6]. These laser systems are mostly based on amplification of chirped pulses [1, 2] using either laser amplifiers or non-storage optical parametric amplifiers termed as chirped pulse amplification (CPA) or optical parametric chirped pulse amplification (OPCPA) techniques respectively. Energy or power scaling of any CPA/OPCPA based laser systems is often limited [7–19] by the size and desired specification of the pulse compression gratings (*e.g.* damage threshold, diffracted wavefront distortions, weight for handling requirement etc). To avoid some of these limitations, two or more gratings are phase locked [7] in such a way that a tiled grating assembly (TGA) mimic a monolithic grating. Two or more such tiled grating assemblies are used to build a large aperture laser pulse compressor to achieve energetic ultra-short laser pulses. In most of practical situations, TGA is often trade off with large size expensive gratings with desired specification in terms of compressed pulse parameters [8, 9]. Two regimes of tiled pulse compressor depending upon desired pulsed beam fidelity have been reported in the literature, one mimic multi-beamlet compressors with and without diffraction effects and other

mimic spectral filter generating temporal pedestals. For example, three small size gratings (*each* $14 \times 12 \times 2 \text{ cm}^3$) are used in one tiled grating assembly and three such tiled grating assemblies have been incorporated in the pulse compressor of a 50 TW class hybrid Nd:glass laser system [20] at RRCAT Indore. In contrast, one tiled grating assembly consisting of grating of size $70 \times 19 \times 5 \text{ cm}^3$ is used in the compressor of POLARIS laser system [13] at university of Jena, Germany. Detection of various phase errors (*angular: tip, tilt and in-plane rotation; linear: longitudinal and lateral translation*) and grating groove density errors is desirable to maintain any tiled laser pulse compressor operating in any regime to achieve desired characteristics of pulsed beam in terms of spatial and temporal parameters (*e.g.* far-field focal spot, pulse duration, pulse contrast, etc).

Different phase locking techniques are reported to achieve beam-locking or optic-locking of the tiled optic assemblies *e.g.* grating assemblies of pulse compressors, mirror assemblies of telescopes etc. These techniques are primarily based on far field spatial beam profilometry [21–30], interferometry [8–19], and imaging principles [31, 32]. Most of techniques use either spectrally broadband beam or a monochromatic beam (*single or multiple*) at same or different wavelengths to avoid ambiguities in the phase detection. Use of separate cw laser beam at different spectral frequencies is an early and well accepted technique used to align laser pulse compressors

independently before actual compression laser shot (*e.g. pulse compressor at central laser facility in UK*) and also in the case of tiled assemblies consisting of two or more gratings, often in-situ conditions for real time detection and correction of various phase errors. Next, depending upon experimental requirements, hybrid methods consisting of two or more alignment techniques based on different principles in different optical geometries are chosen. Grating assemblies, in contrast to non-angular dispersive optic assemblies, require monitoring of both reflected and diffracted beams for phase errors together with interferogram. Since it is desirable to monitor profiles of both reflected and diffracted beams together with interferometry for each TGA of pulse compressor, diagnostic system become practically cumbersome in some situations to allow monochromatic beam for probing various phase errors of a tiled pulse compressor in the presence of actual broadband laser beam. Next, ambiguity in estimation of linear displacements (*modulo of π in double pass*) using monochromatic source necessitate either use of two-wavelength measurements or use of mechanical switches to limit actuation or require monitoring of fringe visibility or peak of interferogram of cw or pulsed broadband sources to avoid temporal de-synchronization errors dictated by the desired compressed pulse duration. In contrast, application of spectrally broadband aberration free pulsed laser beam itself, often available in the case of CPA laser systems, to monitor phase errors of TGA shall reduce experimental complexity. Further, operation and maintenance of a laser pulse compressor [19, 33–36], one also need to estimate groove density of the grating in situations requiring re-placement of any grating of compressor. Therefore, it is desirable to built phase detection and correction diagnostic system to avoid above mentioned limitations. In this paper, a simple intra-beam diagnostic system has been proposed for aligning tiled planar optics, primarily based on spatial and spectrally resolved far-field profilometry coupled with spatio-spectral interferometry with enhanced precision. Present diagnostic system has been applied to detect and correct angular and piston errors of a tiled two-grating assembly (TTGA) without any ambiguity and to estimate groove density errors of gratings of the given assembly. Since spatial and temporal de-synchronization errors of pulse compressor stage are monitored using low power reflected beam from first grating of the pulse stretcher, applicability of present setup is demonstrated to phase lock pulse compressor independently prior to main laser pulse compression shot. Further, present technique does not require either mechanical switch to limit actuation or another spectrally broadband source to remove ambiguity in phase errors to desired accuracies [19]. Experimental results are reported for a TTGA based Treacy laser pulse compressor using a cw mode-locked femtosecond Nd:glass based laser oscillator delivering ~ 200 fs duration laser pulses at 100 MHz.

2. Experimental setup

Figure 1 depicts a typical experimental setup of TTGA based tiled grating laser pulse compressor coupled with diagnostics for detection and correction of phase errors of TTGA. Pulse compressor consists of a monolithic grating, G_1 , and two-gratings, G_{21} and G_{22} , tiled assembly and retro-mirror, RM to allow different optical path for forward (*incident*) and backward (*diffracted*) beams to be intercepted by the pickup mirror as pictorially illustrated. While groove density of gratings is ~ 1740 lines mm^{-1} , size of the gratings used in TTGA is $110 \times 80 \times 10$ mm^3 . Gratings of TTGA are placed on mechanical stage consisted of two Newfocus 9081 aligner stages kept on in-house fabricated tilt stage to achieve tip, tilt, in-plane rotation and longitudinal/lateral piston, while first grating of compressor is housed on another Newfocus 9081 aligner stage. Three diagnostics namely spatio-spectral interferometer, profile-monitors, and point diffraction interferometer used to diagnose phase errors of TTGA with varying precision are shown in figure 2a–c, respectively. In addition, near-field spatial interferometer for cross-beam interference using two-mirror in reflective bi-prism geometry (figure 1) has also been used for detection of phase errors of TTGA. In this case, two mirrors in reflective bi-prism geometry have been used in such a way that optical arrangement does not introduce any temporal delay between the beam-lets.

Laser beam from the femtosecond laser oscillator (GLX 200 from Time Bandwidth Products) is allowed to travel through compressor and reflected, diffracted beams from first grating and TTGA of compressor are picked up to generate far-field spatial profiles required to monitor various errors of TTGA. While both reflected beams one from TTGA, collected using cylindrical and spherical lenses while travelling through mirrors M_1 , M_2 to record spectrally resolved far field profiles, and other from first grating G_1 , collected using a plano-convex lens SL while traversing through mirrors M_3 , M_4 are allowed to incident on a detector screen, diffracted beam from tilted grating assembly is allowed to incident on inverting spatial-spectral interferometer to generate spatial-spectral interferogram on the detector screen used for far-field profiles of the beams as shown in figure 1.

Reflected and diffracted beam-lets from TTGA are also collected using spherical lens using set of folding mirrors M_5 , M_6 , M_7 to obtain far-field profile on common detector screen. Suitable neutral density filters have been used to equalize intensity of laser beams i.e. interfering and reflected beams etc for faithful recording by the CCD camera. Since far-field profiles and interferograms are displayed on single detector screen, which is imaged on to single 8 bit CCD camera (*Watec 902B*), complexity of electronics used in near simultaneous image acquisition in the case of multiple cameras is greatly reduced on the cost of reduced spatial resolution. Additional CCD camera has

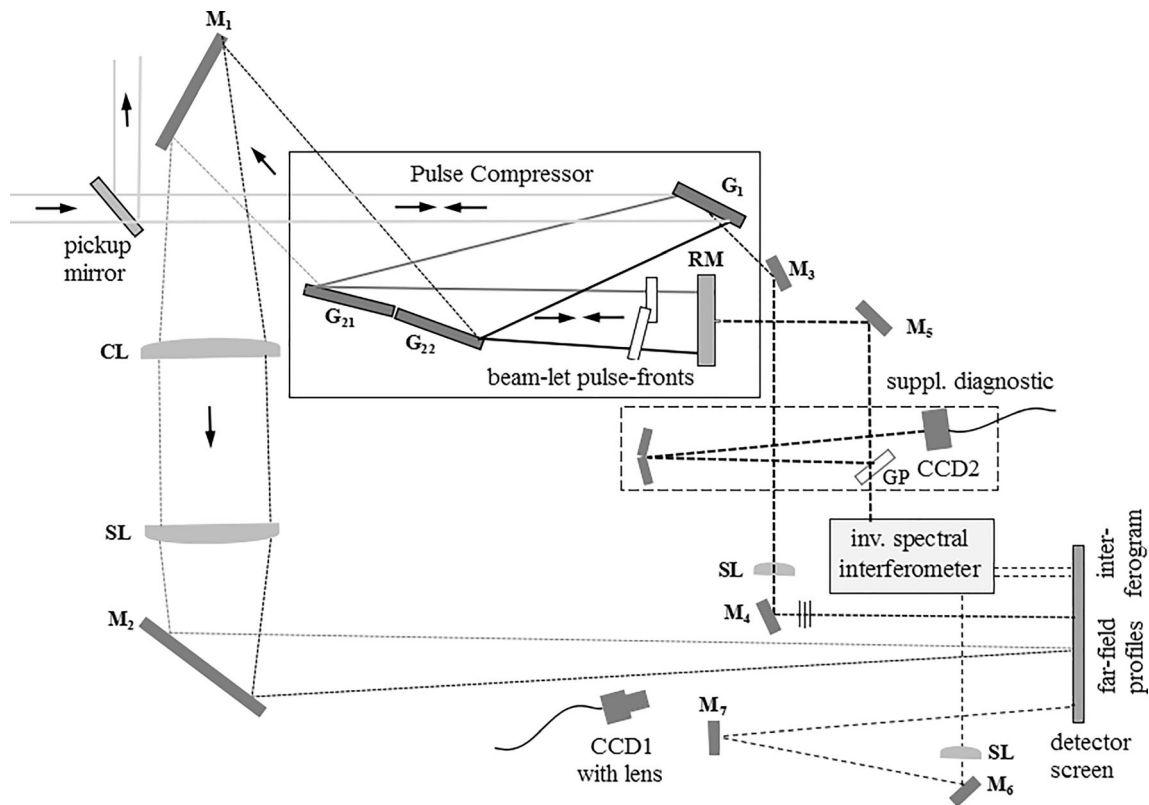


Figure 1. Typical setup of tiled grating laser pulse compressor coupled with diagnostics for detection and correction of phase errors of TTGA.

been used for recording of a spatial interferogram between beam-lets from TTGA as clearly illustrated in figure 1. Video signals from CCD cameras are digitized using National Instrument video frame grabber card NI1410 through multiplexer A6822 to allow monitoring and processing of far field intensity distribution of reference, reflected and diffracted beams, spatial and spatio-spectral interferogram of the leaked beam through one of mirror of retro-reflector of pulse compressor. Following procedure has been adapted to phase lock TGA. First, angular errors of reflected and diffracted beams are minimized by using point diffraction interferometer and then far-field profilometry coupled with spectral interferometry is applied to detect and correct angular and piston errors of TGA. While spectrally resolved reflected beam far-field profilometry has been used mainly for tip and in-plane rotation errors, diffracted beam far-field spatial profiles coupled with spatio-spectral interferograms have been used to avoid ambiguity in paired variables of the different phase errors. Any deviation in diffraction angle of beam-lets in three-dimensional space from TGA, arising either due to tilt or inter-groove density error of TGA, or due to tip or in-plane rotation error, results in varying spectral shifting and temporal delay between two beams of inverting spectral interferometer causing variation in interferogram (*e.g. fringe visibility, frequency and rotation*). Further, piston

error of TGA also cause variation in temporal delay between two halves of the inverting spectral interferometer. Therefore, angular and piston errors of TGA can be easily monitored and corrected with sub-wavelength accuracies without ambiguity. Mismatch in groove density of the gratings of TTGA can also be monitored over limited range without re-optimization of the experimental setup, which in turn help ease in operation and maintenance of compressor requiring re-placement of any grating.

In contrast, phase errors of tiled optic assembly (TOA) can be detected by monitoring pattern and visibility of spatial fringes. For instance, maximizing fringe visibility of the spatial interferogram ensure near zero piston error, thus necessitating a spectrally broadband source [19] to reduce phase error of TOA to desired accuracies in general. For comparison typical spatial-spectral and spatial interferograms are given in figure 2(d) and discussed later in the next Section. However, it is mentioned that spatial interferograms are recorded within coherence length of the laser beam, which is $\sim 60 \mu\text{m}$ in the present case, ensuring matching of two halves within fraction of this length, sufficient for de-synchronization issues of compressor. Spectrally broadband source is needed for enhanced precision except in the case of temporal interferograms and generally available for much shorter duration CPA laser systems. Next, single focal spot of compressed beam can be obtained

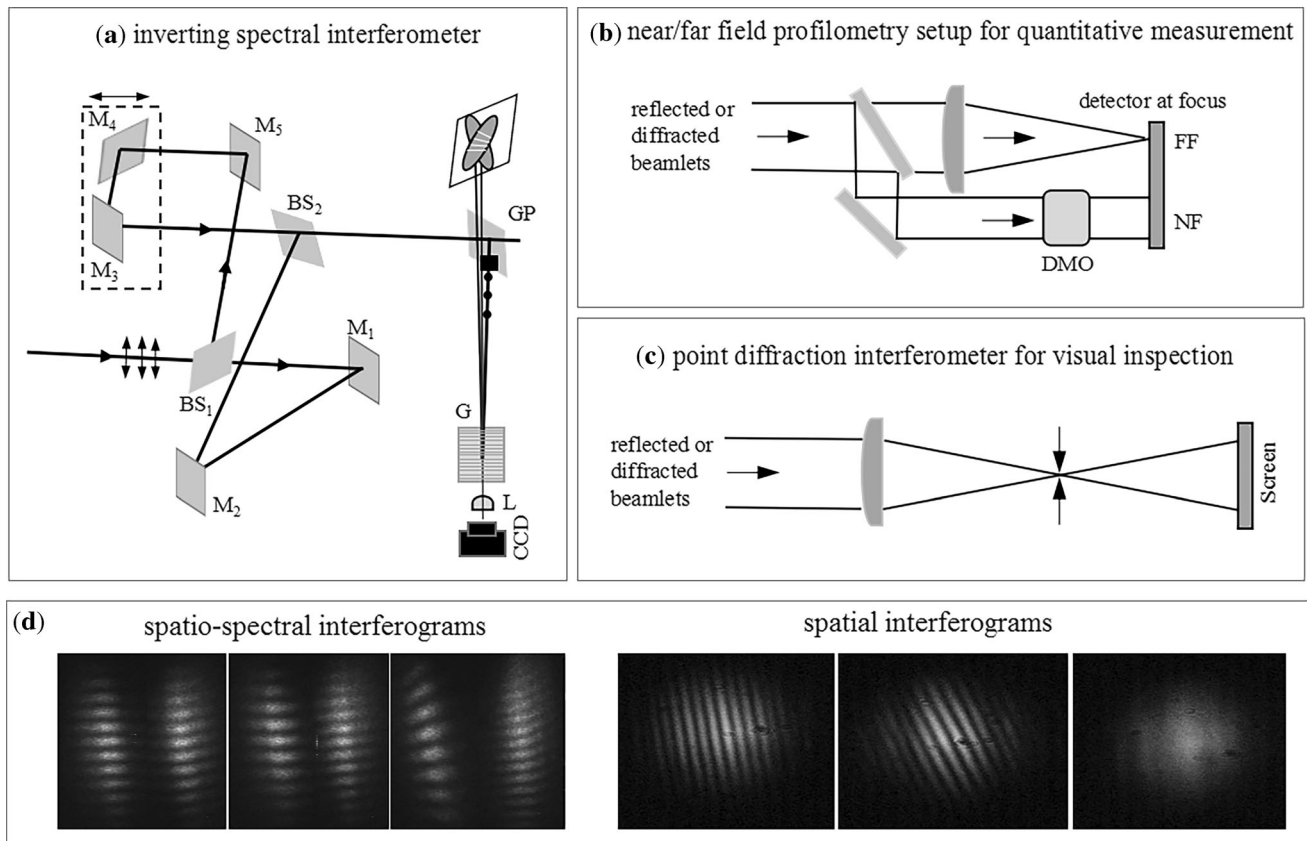


Figure 2. Typical setup of various diagnostics of TGA based on: (a) spatio-spectral interferometry, (b) far field profilometry, (c) point diffractometry, and (d) Typical spatio-spectral (left) and spatial interferograms (right) under different phase errors of tiled pulse compressor. No fringe visibility (extreme right image) in case of spatial interferogram for delay larger than coherence length.

simply using tip/tilt correction within or outside the disperser.

3. Experimental results

Different examples have been chosen to demonstrate phase locking of TTGA [19, 36] and a composite image has been generated, for each example shown in respective figure, to include spatio-spectral interferograms (*top-left*), spectral power density of full interferogram (*top-middle*), combined power spectral density of individual interferograms (*top-right*), spectrally resolved far-field profile (*middle*), and far-field spatial profiles of referenced, reflected and diffracted beams (*bottom*). Referenced black lines are also shown in far-field profiles of reflected and diffracted beams for visual identification of phase error of TTGA (e.g. *single slope of locus of maxima of spectrally resolved profile represents negligible tip or in-plane rotation error*). Next, it is stated that far-field profiles of two halves of the laser beam from spectral interferometer (*although one is sufficient for angular error detection*) are shown in each example to

retrieve information of interaction geometry of the interferometer.

Figure 3 depicts typical composite images obtained under different values of angular errors (*tilt, tip, and in-plane rotation*) and linear translation errors (*longitudinal, lateral*) of the TTGA. An example of dominant piston is given in figure 3(a). Captions are also embedded in this figure and are applicable for all composite images. It may be seen clearly from this example that spectral fringe frequency of two halves of interferogram is different owing to different temporal delay caused by the piston error of TTGA. Both magnitude and sign of piston error of TTGA can be estimated without ambiguity for known temporal delay between two beam-lets of the inverting spectral interferometer. Using fringe frequency equalization for two halves of the interferograms, relative temporal delay between two interfering beams (*hence piston error of TTGA*) can be easily minimized to zero as illustrated. However, in practical condition estimating absolute fringe frequencies (*hence absolute path difference*) depends on spectral resolution of spectrograph, number of spectral points which can also be enhanced digitally and has been demonstrated earlier with accuracies of few wavelengths.

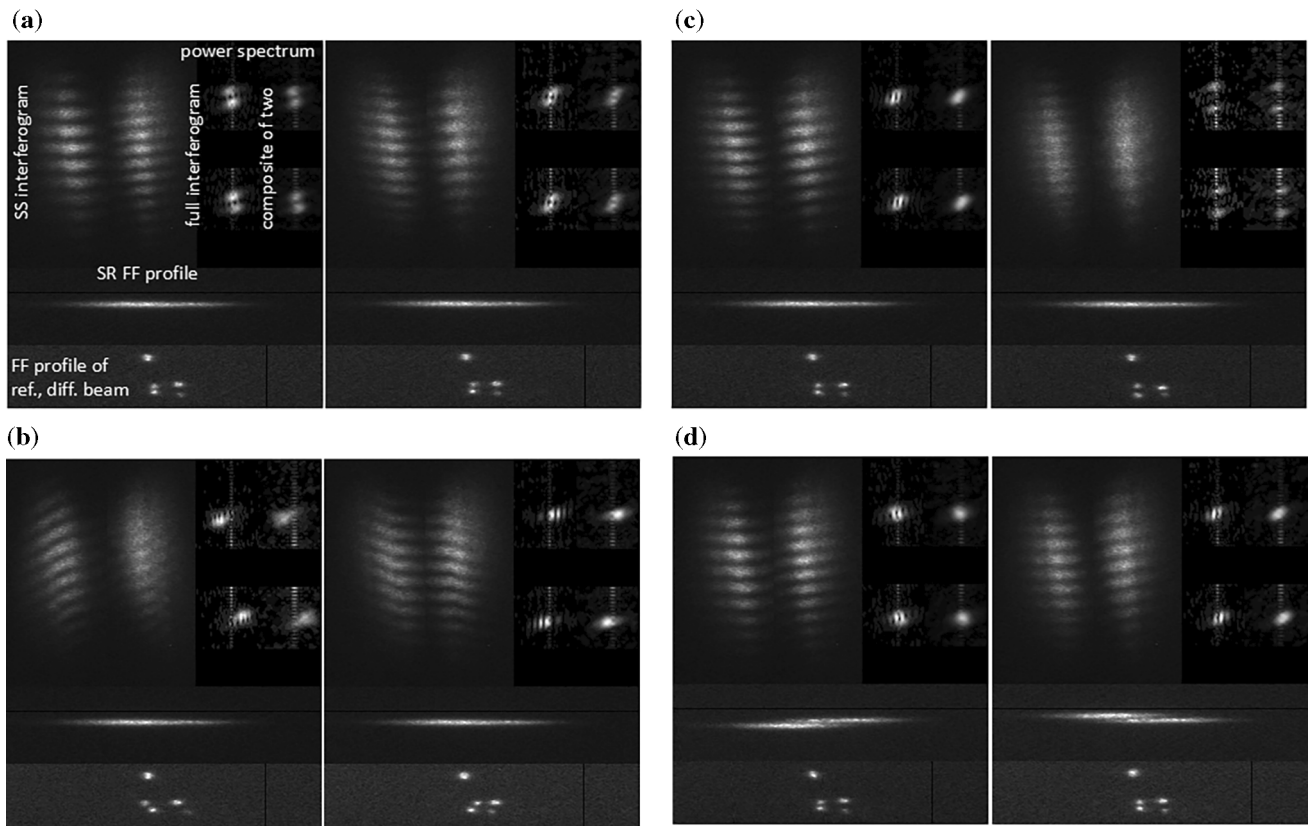


Figure 3. Typical composite image of measurements corresponding to different amounts of phase errors: (a) dominant piston, (b) dominant tilt, (c) dominant in-plane rotation error and (d) dominant tip error corrected using in-plane rotation and piston. Referenced horizontal and vertical black lines are also shown in spectrally resolved profile of reflected beam and far-field profiles of reflected/diffracted beams respectively for visual identification of angular errors. Caption for each measurement is given in 3(a).

Further, differential phase shifts of the interferograms provide estimation of piston with sub-wavelength accuracies. However, it is mentioned that such precision is not required in the pulse compression experiments involving multi-cycle duration laser pulses except phase locking to obtain single focal spot. Next, far-field spatial profiles of diffracted and reflected beams, shown in respective composite image, also indicated negligible angular error of TTGA in the present case. Further, space resolved spectral interferograms also help to minimize angular errors of TGA as offset fringe carrier owing to differential temporal delay across beam. An example of dominant tilt is given in the figure 3(b), which show composite image of different measurements for two values of the tilt. Varying tilt angle cause rotation of spectral fringes as illustrated for two different values of tilt error of opposite sign. Spectral power density of full and individual interferograms and far-field profiles of the diffracted beam (*two different focal spots*) also indicate different values of tilt error of the TTGA relative to fixed grating. Next, examples of TTGA with tip and in-plane rotation (IPR) errors are considered. While tip error cause equal beam pointing errors in both reflected and diffracted beams, IPR error affect diffracted beam only.

Therefore, simultaneous monitoring of far-field profiles of diffracted and reflected beams allow visual identification of tip in presence of IPR. Further, change in pointing of diffracting beam in either direction (*owing to tip or IPR errors*) cause spectral shifting of the two halves of the inverting spectral interferometer leading to smaller visibility of spectral fringes and can be easily detected in spatio-spectral interferometry as well. Examples of TTGA with dominant tip and in-plane rotation errors are illustrated respectively in the figure 3(c) and (d) for two different values of opposite sign around phased condition. Visibility of the spectral fringes is observed to decrease, as expected, with tip or in-plane rotation errors. Further, spectral fringe frequency of the two halves of the interferogram is also observed to vary with angular errors and is attributed to relative temporal delay between beam-lets caused owing to e.g. non-gimbal mounts housing TGA. Coupled with far-field profilometry, ambiguity in paired variables of TGA are also avoided. For instance, while angular errors cause spectrally dispersed far-field profile owing to residual angular dispersion and spatial chirp, tip/tilt error cause eventual splitting of far-field profiles in vertical/ horizontal directions prior to variation in intensity distribution

(ensuring sub-wavelength precision). Next, since phase error of TGA are obtained from differential angular errors of the interfering beams and far-field profiles, it is important to monitor angular errors of the beams due to interferometer setup. From these illustrations, it may be seen clearly that different angular errors of TGA can be detected and corrected with sub-wavelength accuracies. Further, piston error of TTGA can also be estimated with sub-wavelength accuracies without 2π ambiguity, that normally occur in most of cases using monochromatic or broadband sources.

Next, in addition to realizing phased array of gratings of tiled pulse compressor, aligning and maintaining tiled pulse compressor remain another task. For example, any deviation between diffraction angle at first grating (or TGA) and incidence angle at second grating (or TGA) shall result in generation of spectral divergence or pulse front tilt in the beam (*or beam-lets*). Therefore, monitoring of angular divergence (*or PFT*) of beam (*or beam-lets in case of tiled pulse compressor*) help easier identification and correction of phase error of pulse compressor without using any additional optics. Example with nearly well aligned tiled pulse compressor with phased array of gratings is depicted in figure 4(a), while misaligned tiled pulse compressor with non-phased array of gratings is shown in figure 4(b) corresponding to two different tilt values of the TTGA relative to a first grating of the pulse compressor. For misaligned compressor, far-field profiles (also power spectra of spatio-spectral interferogram) are dispersed owing to angular dispersion and spatial chirp as shown in this example. From this illustration, it is stated that both spatio-spectral interferogram and far-field profiles may be applied to detect and correct phase error of array of grating and pulse compressor. TGA, however can also be phased in such cases by equalizing value of angular dispersion estimated from two halves of the spatio-spectral interferograms.

Now, in the case of tiled pulse compressor, a situation may occur in practice where TGA has gratings with groove density deviated from the designed values due to various reasons e.g., gratings from two different manufacturers fabricated under different conditions. Such grating assemblies are not desirable for faithful laser pulse compression owing to residual uncompensated angular dispersion caused by grating groove-density mismatch, although inter-groove density errors of TGA may be tolerated to some extent [35] owing to tilt as one of degree of freedom of tiled pulse compressor. Examples of TGA with inter-groove density errors has been considered to illustrate detection of such practical situations. Since tilt error of TTGA is paired with inter-groove density error of TGA, any deviation in groove spacing between two gratings results in different beam pointing of the diffracted beam causing ambiguity in estimation of tilt error of TTGA. However, simultaneous monitoring of far-field profiles avoid this ambiguity and is taken as an advantage to test any grating of TGA for inter-groove density errors in order to replace any grating of TGA for easier operation and maintenance of the tiled pulse compressor. Figure 5(a) and (b) present composite images of various measurements corresponding to TTGA consisting of gratings [36] with inter-groove density (ΔN) error of $0.03 \text{ lines mm}^{-1}$ and $4.75 \text{ lines mm}^{-1}$ respectively. Far-field profiles of reflected beam from TTGA is also shown along with spectrally resolved far-field profiles. From spatio-spectral interferograms shown in figure 5(a) corresponding to TTGA with smaller inter-groove density errors, it may be noticed that there remain relative tilt error causing rotation of fringes in one half of the interferogram, while diffraction angle detector did not show visual presence of tilt error. This is in contrast to measurements given for TTGA with larger inter-groove density errors (figure 5(b)), where-in a large difference in angle of incidence is

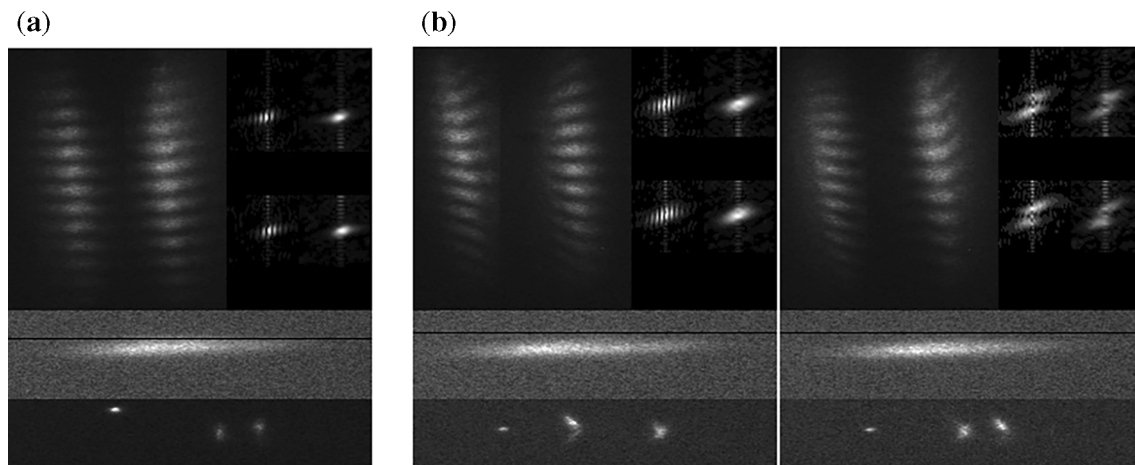


Figure 4. Typical composite image of measurements corresponding to: (a) aligned compressor with phase matched gratings and (b) misaligned compressor with different tilt angles. Dispersed far-field profiles and power spectra of interferogram indicate misalignment.

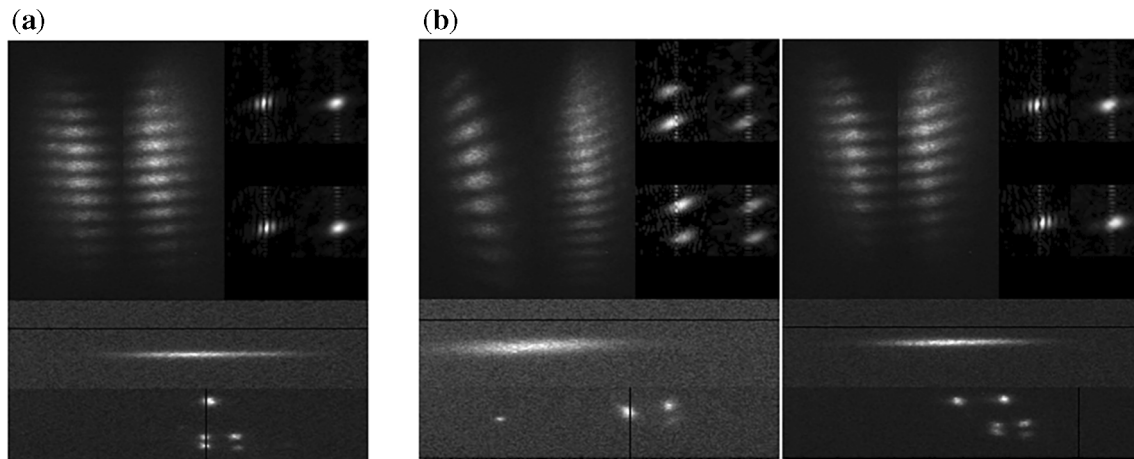


Figure 5. Typical composite image of measurements corresponding to grating with different groove densities: (a) $\Delta N = 0.03$ lines mm^{-1} and (b) $\Delta N = 4.75$ lines mm^{-1} for different alignment conditions.

observed for nearly equal diffraction angles at central wavelength as inferred from far-field profilometry coupled with interferograms. Further, example of misaligned compressor presented in figure 5(b), also show generation of angular dispersion and spatial chirp as clearly seen from respective interferometry and far-field profilometry data. From this illustration of a near-phase matched TTGA (*in terms of diffracted beams*) shown in figure 5(b), the difference in angle of incidence in the case of TTGA with different gratings is estimated to be $\sim 0.61^\circ$ using far-field profiles of reflected beam from TTGA, which corresponds to inter-groove density (ΔN) error of 4.85 lines mm^{-1} at wavelength of 1056 nm.

From above illustration using various examples of phase errors of TTGA, it is stated that different linear and angular errors of TGA can be detected and corrected with sub-wavelength precision without ambiguities. It is further stated that no-attempt was done to improve precision in various measurement in a demonstrating experiment. However, it is mentioned that present experiment, carried out using laser beam with 10 mm diameter (*natural divergence of ~ 134 μrad*), also allow estimation of angular errors of ~ 10 μrad in sparrow criteria, which is smaller than Rayleigh diffraction limit owing to multi-thresholding technique applied in detection of centroids of far-field spatial profiles. Accuracies in estimating angular errors can also be significantly improved either by using a large size beam of desired wavefront quality or using a simultaneous dual interferometric measurements at extremities of the gratings using smaller low power beam with higher wavefront quality. And angular scaling achieved through optimized interaction geometry also helps to achieve higher precision in the angular errors measurement in spatio-spectral interferometry as well. Ambiguity in paired variables of TTGA (e.g. *tip with ipr error, tilt with groove density error*) is removed by simultaneous

monitoring beam pointing of both reflected and diffracted beams, as illustrated through various examples of phase errors of TTGA. Electronically controlled actuators to generate tilt, tip, in-plane rotation and piston movements using a referenced beam, required for automatic phase locking of TGA and tiled pulse compressor as whole, will further improve accuracies in estimation and correction of various phase errors.

4. Conclusion

In summary, a simple intra-beam alignment setup, primarily based on spatial and spectrally resolved far-field profilometry coupled with interferometry with enhanced precision, has been demonstrated to phase lock tiled grating assemblies, aligning and maintaining a tiled grating laser pulse compressor. Both linear and angular errors of tiled two-grating assembly are detected and corrected with sub-wavelength accuracies without ambiguity, independently using low power pulsed beam with high wavefront quality from first grating of the pulse stretcher, prior to main laser pulse compression shot. Inter-groove density errors of tiled grating assembly are also estimated. Further, use of either monochromatic laser beams of different wavelengths or spectrally broadband cw source to remove ambiguity in piston errors to the desired accuracies are also avoided.

References

- [1] Strickland D and Mourou G 1985 Compression of amplified chirped optical pulses. *Opt. Commun.* 56: 219–221
- [2] Dubeietis A, Jonusauskas G and Piskarskas A 1992 Powerful femtosecond pulse generation by chirped and stretched pulse

- parametric amplification in BBO crystal. *Opt. Commun.* 88: 437–440
- [3] Zuegel J D, Borneis S, Barty C P J, Legarrec B, Danson C, Miyanaga N, Rambo P K, Leblanc C, Kessler T J, Schmid A W, Waxer L J, Kelly J H, Kruschwitz B, Jungquist R, Moses E, Britten J, Jovanovic I, Dawson J and Blanchot N 2006 Laser challenges for fast ignition. *Fusion Sci. Technol.* 49: 453–482
- [4] Leemans W and Esarey E 2009 Laser-driven plasma-wave electron accelerators. *Phys. Today* 62(3): 44–49
- [5] Kumar R G 2009 Intense ultrashort light and dense matter. *Pramana* 73(1): 113–155
- [6] Brenner C M, Mirfayzi S R, Rusby D R, Armstrong C, Alejo A, Wilson L A, Clarke R, Ahmed H, Butler N M H, Haddock D, Higginson A, McClymont A, Murphy C, Notley M, Oliver P, Allott R, Hernandez-Gomez C, Kar S, McKenna P and Neely D 2016 Laser-driven X-ray and neutron source development for industrial applications of plasma accelerators. *Plasma Phys. Control. Fusion* 58: 014039
- [7] Zhang T, Yonemura M and Kato Y 1998 An array-grating compressor for high-power chirped-pulse amplification lasers. *Opt. Commun.* 145: 367–376
- [8] Blanchot N, Bar E, Behar G, Bellet C, Bigourd D, Boubault F, Chappuis C, Coic H, Dupont C D, Flour O, Hartmann O, Hilsz L, Hugonnot E, Lavastree E, Luce J, Mazataud E, Neauport J, Noailles S, Remy B, Sautarel F, Sautet M and Rouyer C 2010 Experimental demonstration of a synthetic aperture compression scheme for multi-Petawatt high-energy lasers. *Opt. Exp.* 18: 10088–10097
- [9] Kessler T J, Bunkenburg J, Huang H, Kozlov A and Meyerhofer D D 2004 Demonstration of coherent addition of multiple gratings for high-energy chirped-pulse-amplified lasers. *Opt. Lett.* 29: 635–637
- [10] Harimoto T 2004 Far-field pattern analysis for an array grating compressor. *Jpn. J. Appl. Phys.* 43(4A): 1362–1365
- [11] Bunkenburg J, Kessler T J, Skulski W and Huang H 2006 Phase-locked control of tiled-grating assemblies for chirped-pulse-amplified lasers using a Mach-Zehnder interferometer. *Opt. Lett.* 31: 1561–1563
- [12] Blanchot N, Marre G, Néauport J, Sibe E, Rouyer C, Montant S, Cotel A, Le Blanc C and Sauteret C 2006 Synthetic aperture compression scheme for a multipetawatt high-energy laser. *Appl. Opt.* 45(23): 6013–6021
- [13] Hornung M, Bodefled R, Siebold M, Schnepf M, Hein J, Sauerbrey R and Kaluza M C 2007 Alignment of a tiled-grating compressor in a high-power chirped-pulse amplification laser system. *Appl. Opt.* 46: 7432–7435
- [14] Cotel A, Castaing M, Pichon P and Le B C 2007 Phased-array grating compression for high energy chirped pulse amplification lasers. *Opt. Exp.* 15: 2742–2752
- [15] Qiao J, Kalb A, Guardalben M J, King G, Canning D and Kelly J H 2007 Large-aperture grating tiling by interferometry for petawatt chirped pulse amplification systems. *Opt. Exp.* 15: 9562–9574
- [16] Hornung M, Bodefled R, Kessler A, Hein J and Kaluza M C 2010 Spectrally resolved and phase-sensitive far-field measurement for the coherent addition of laser pulses in a tiled grating compressor. *Opt. Lett.* 35: 2073–2075
- [17] Habara H, Xu G, Jitsuno T, Kodama R, Suzuki K, Sawai K, Kondo K, Miyanaga N, Tanaka K A, Mima K, Rushford M C, Britten J A and Barty C P J 2010 Pulse compression and beam focusing with segmented diffraction gratings in a high-power chirped-pulse amplification glass laser system. *Opt. Lett.* 35: 1783–1785
- [18] Hernandez-Garcia C, Mendez C, Arias I, Vazquez de Aldana J R, Varela O, Sola I J and Roso L 2012 Role of longitudinal piston error in tiled grating compressor in second and higher order harmonic generation. *Appl. Phys. B* 108: 773–777
- [19] Sharma A K, Joshi A S, Naik P A and Gupta P D 2017 Active phase locking of a tiled two-grating assembly for highenergy laser pulse compression using simultaneous controls from far-field profiles and interferometry. *Appl. Phys. B* 123: 117
- [20] Joshi A S, Kamath M P, Sharma A K, Raghuramaiah M, Patidar R K, Ansari M S, Sreedhar N, Chandra R, Navathe C P, Naik P A and Gupta P D 2013 Development of a two arm, high energy, high power laser for plasma research in India. *EPJ Web of Conferences* 59: 08001–08004
- [21] Chanan G A, Troy M, Dekens F, Michaels S, Nelson J, Mast T and Kirkman D 1998 Phasing the mirror segments of the Keck telescopes: the broadband phasing algorithm. *Appl. Opt.* 37: 140–155
- [22] Chanan G A, Ohara C and Troy M 2000 Phasing the mirror segments of the Keck telescopes II: the narrow-band phasing algorithm. *Appl. Opt.* 39(25): 4706–4714
- [23] Zeng L and Li L 2006 Method of making mosaic gratings by using a two-color heterodyne interferometer containing a reference grating. *Opt. Lett.* 31(2): 152–154
- [24] Hu Y and Zeng L 2007 Grating mosaic based on image processing of far-field diffraction intensity patterns in two wavelengths. *Appl. Opt.* 46(28): 7018–7025
- [25] Hu Y, Zeng L and Li L 2007 Method to mosaic gratings that relies on analysis of far-field intensity patterns in two wavelengths. *Opt. Commun.* 269: 285–290
- [26] Guo C and Zeng L 2008 Measurement of period difference in grating pair based on analysis of far-field intensity patterns. *Opt. Commun.* 281: 3611–3616
- [27] Guo C and Zeng L 2009 Measurement of period difference in grating pair based on compensation analysis of phase difference between diffraction beams. *Appl. Opt.* 48(9): 1651–1657
- [28] Shi L, Zeng L and Li L 2009 Fabrication of optical mosaic gratings with phase and altitude adjustments employing latent fringes and a red-wavelength dual-beam Interferometer. *Opt. Exp.* 17(24): 21530–21543
- [29] Yang Y, Wang X, Zhang J, Luo H, Li F, Huang X and Jing F 2011 Demonstration of state-locked control of tiled system. *Opt. Engg.* 50(9): 093601–093606
- [30] Yang Y, Wang X, Zhang J, Luo H, Li F, Huang X and Jing F 2012 Automatic phase-locked control of grating tiling. *Opt. Las. Eng.* 50: 262–267
- [31] Salinas-Luna J, Luna E, Salas L, Cruz-Gonzalez I and Cornejo-Rodríguez A 2004 Ronchi test can detect piston by means of the defocusing term. *Opt. Exp.* 12(16): 3719–3736
- [32] Jeong J, Lee B and Lee S 2010 Determination of paraxial image plane location by using Ronchi test. *Opt. Exp.* 18(17): 18249–18253

- [33] Gurardalben M J 2008 Littrow angle method to remove alignment errors in grating pulse compressors. *Appl. Opt.* 47(27): 4959–4964
- [34] Li Z, Wang T, Xu G, Li D, Chen L and Dai Y 2013 Littrow angle based autocollimation method for precision online monitoring three-dimensional angular drifts of chirped-pulse compression-gratings. *Rev. Sci. Instrum.* 84: 63109–63117
- [35] Rushford M C, Britten J A, Barty C P J, Jitsuno T, Kando K, Miyanaga N, Tanaka K A, Kodama R and Xu G 2008 Split-aperture laser pulse compressor design tolerant to alignment and line-density differences. *Opt. Lett.* 33(16): 1902–1904
- [36] Sharma A K and Joshi A S 2019 On the estimation of absolute grating groove density and inter-grating groove density errors of laser pulse compression gratings. *Sadhana* 44(3): 59